

Review Article

A Cutting-Edge Survey of Tribological Behavior Evaluation Using Artificial and Computational Intelligence Models

Senthil Kumaran Selvaraj ¹, Aditya Raj ², Mohit Dharnidharka ¹, Utkarsh Chadha ¹,
Isha Sachdeva ², Chinmay Kapruan ¹ and Velmurugan Paramasivam ³

¹Department of Manufacturing Engineering, School of Mechanical Engineering (SMEC), Vellore Institute of Technology (VIT), Vellore, Tamilnadu 632014, India

²School of Information Technology and Engineering (SITE), Vellore Institute of Technology (VIT), Vellore, Tamilnadu 632014, India

³School of Mechanical and Automotive Engineering, College of Engineering and Technology, Dilla University, P.O. Box 419, Dilla, Ethiopia

Correspondence should be addressed to Senthil Kumaran Selvaraj; senthilkumaran.s@vit.ac.in and Velmurugan Paramasivam; drvelmuruganp@du.edu.et

Received 28 October 2021; Revised 14 December 2021; Accepted 16 December 2021; Published 29 December 2021

Academic Editor: Ali Khorram

Copyright © 2021 Senthil Kumaran Selvaraj et al. This is an open access article distributed under the Creative Commons Attribution License, which permits unrestricted use, distribution, and reproduction in any medium, provided the original work is properly cited.

Any metal surface's usefulness is essential in various applications such as machining and welding and aerospace and aerodynamic applications. There is a great deal of wear in metals, used widely in machines and appliances. The gradual loss of the upper metal layers in all metal parts is inevitable over the machine or component's lifetime. Artificial intelligence implementations and computational models are being studied to evaluate different metals' tribological behavior, as technological progress has been made in this field. Different neural networks were used for different metals. They are classified in this paper, together with a description of their benefits and inconveniences and an overview and use of the different types of wear. Artificial intelligence is a relatively new term that uses mechanical engineering. There is still no scientific progress to examine various metal wear cases and compare AI and computational models' accuracy in wear behavior.

1. Introduction

Given the potential and technological developments we have experienced in an industrial revolution, we have a long path to cover as engineers. The wear behavior varies from metal to metal, mainly depending on its properties or the method used, and AI has helped companies better understand metals' wearing behavior and deploy them in processes or machinery because the speed with precision is more critical in the industry, helping companies increase their response speed. Artificial intelligence is a computer science field dealing with the simulation of computer systems to imitate human intelligence. AI is a large field in computers and other areas such as economics, theory of control, probability, optimization, and bilingualism. AI is such a phenomenon

that it can model and find patterns in complex inputs and outputs on the given data. It has been made an essential element of our lives without even realizing weather prediction, mechanical wear and tear, the probability of different diseases, and many more, as recommended by Netflix and YouTube. An AI process consists of data acquisition and correction to enhance its earlier forecasts over time. Mechanical engineering, as technology helps mechanical design or engineering works, is AI's biggest consumer. All sections of mechanical engineering benefiting highly from AI are robotics, automation, and sensor technology.

Wear means that the substance is consistently removed from or deformed from a solid surface while moving about another substance or fluid. Wear is a natural phenomenon when two bodies are rubbed or slipped. Mechanical and

chemical behavior and combinations of these factors, such as corrosion, erosion, and abrasion, cause wear on the solid surface of the material. Tribology is the wear science involving friction, lubrication, and wear applications and concepts. Wear is an essential characteristic of products that must be carefully examined before producing a product. Other processes such as fatigue, material failure, and loss of functionality cause surface degradation. In the manufacturing industry, wear is a constant inconvenience, and it is expensive because it is causing loss of part and wear deterioration. The wear of the active surfaces, near-surface compositions, and fragmentation leads to wear debris caused by the plastic deformation of metals. The wear waste produced varies between nanometers and thousands. Wear can be correlated with the help of the wear rate. The material mass or volume removed by the sliding distance of each unit is the ratio. The wear volume per unit is usually expressed as a dimensionless entity called the wear coefficient on the unit's sliding distance (K). The wear mechanism is generally considered a negative feature and is unwanted in most practical contexts, but it has many applications. Wear, for example, is affected by processes such as filing, lapping, sanding, and polishing used to create finished surfaces.

They also collected datasets, if provided, software used, benefits, and drawbacks, and all studies referred to for that survey were fully applicable to explain the subject matter of the case studies cited beforehand and cover artificial intelligence and calculation models as shown in Figure 1.

2. Types of Wear

We must first understand the various types of wear before applying artificial intelligence principles to evaluate wear behavior. Wear can occur due to a single mechanism or a complex combination of mechanisms. To solve a wear problem, we must first understand the various wear mechanisms at work. Abrasion or surface deterioration occurs when the force acting on the surface is caused by load stress or friction. When chemical reactions alter a material body's outer layer, the wear mechanisms responsible are adhesion and tribo-oxidation. The sections that follow describe the various types of clothing.

The most common wear process encountered in the industry is abrasive wear. According to reports, abrasion is to blame for 50% of all wear issues. Abrasive wear is the substance loss caused by hard particles being forced against and moved along a solid surface [1]. The wear mechanism that causes abrasive wear is referred to as abrasion (scraping off). Abrasion occurs when a solid body with a rough surface collides with a coupling part with a soft surface. Abrasive wear is classified into two types based on the type of contact and the contact environment.

- (a) Three-body abrasion: A third dimension is included in sliding two surfaces (as shown in Figure 2), hence blaming the third body for material removal from both surfaces (particles are usually assumed the third body).

- (b) Two-body abrasion: This occurs when the hard material on one surface absorbs material from the opposite surface. Two-body abrasion is always possible because the asperities that cause removal on a hard surface can never be removed entirely, even with the most advanced polishing. As a result, wear debris forms between the two sliding surfaces. Long-term two-body abrasive wear causes three-body abrasion, which causes more wear than two-body abrasion.

Three mechanisms commonly cause abrasive wear:

- (1) Ploughing: The displacement of particles away from the wear particles causes the formation of grooves. Ridges form on the edges of the grooves and are removed by abrasive materials moving through them.
- (2) Cutting is the removal of material from a solid surface in the form of primary debris or microchips. This method is similar to traditional machining.
- (3) Fragmentation occurs when the indenting material is removed from the surface, resulting in a localized fracture.

Adhesive wear: This occurs due to the interaction of asperities between two surfaces [2]. Formalized paraphrase adhesion is the wear mechanism that causes adhesive wear (stickiness). It occurs when the compositions of the two metals are incredibly similar. A bond can form because of this compatibility, allowing parts to seize or become cold-welded together (as seen in Figure 3). Because of these bonded sections' swaying and sliding motion, abrasion occurs on the bordering surfaces. Adhesive wear is classified into two types:

- (a) Classifying wear due to relative motion/direct contact between two surfaces along with plastic deformation, leading to transfer of metal debris onto the other metal's surface during wear.
- (b) Cohesive-adhesive forces hold two faces together even when a significant distance separates them. The actual transition could occur.

Surface fatigue: This occurs when the surface of a material is stressed. As a result of this phenomenon, which thermal or mechanical forces can cause, surfaces crack. The fatigue wear caused due to particle detachment is mainly because of cyclic increase of metal surface microcracks (as shown in Figure 4). Each period increases the crack by a small amount until a surface microcrack develops. As a result, large surface cracks develop over time, posing a direct threat to the components.

Corrosive wear/oxidation wear: This material deterioration combines corrosion and wear. It is defined as a wear phase in which materials slide against each other in a corrosive environment. It is a type of material degradation that combines corrosion and wear. It is defined as a corrosive wear process in which materials slide against each other. When there is no sliding, corrosion on the surfaces forms a micrometer-thick film layer, reducing or even preventing further corrosion. This film is chipped away during the sliding application, exposing the metal surface to further corrosion (as shown in Figure 5). This process of wear occurs in the presence of harmful or

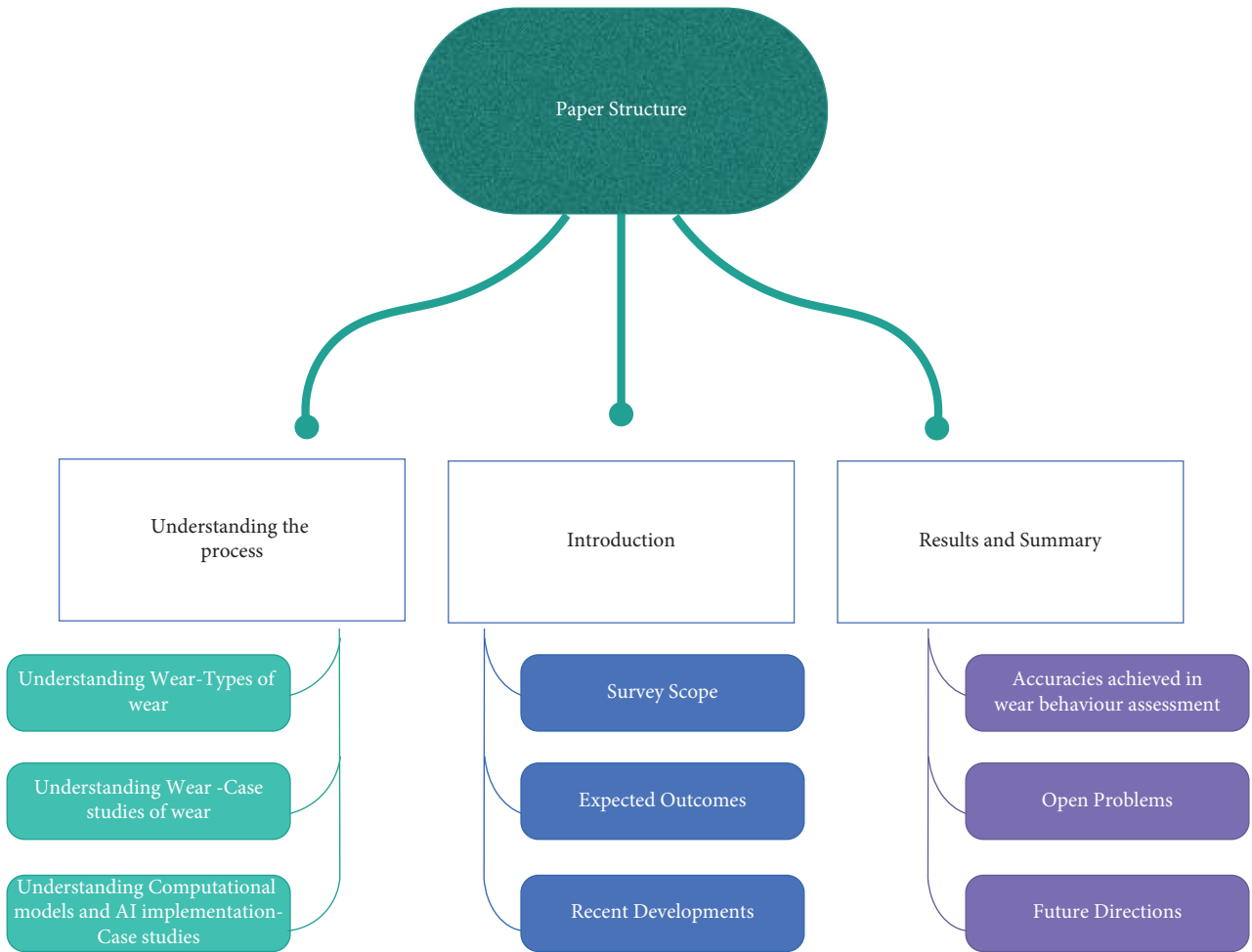


FIGURE 1: Structure of the survey paper.

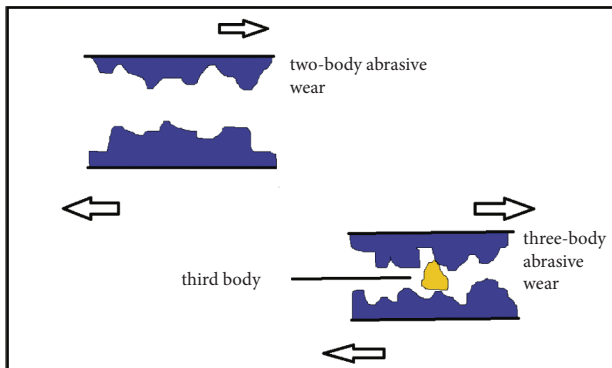


FIGURE 2: Two-body and three-body abrasive wear.

oxidizing metals. Oxidation, also known as rust, is a severe form of corrosive wear. Oxides create a decrease in the equilibrium of friction between surfaces or are often a more significant challenge to work with than the materials involved and can be used as excellent abrasives.

Cavitation wear: A liquid medium causes cavitation wear on metal surfaces. It happens when cavities in a liquid flowing near the material are nucleated, developed, and violently collapsed repeatedly. Because of the rapid changes

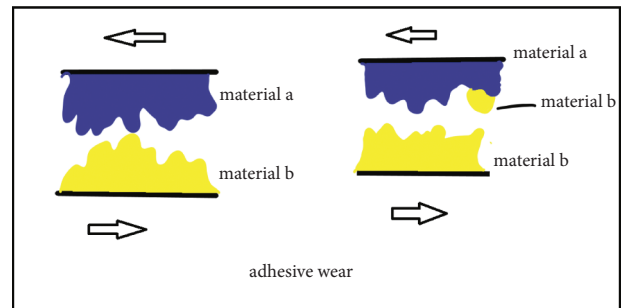


FIGURE 3: Adhesive wear.

in liquid pressure, small vapor-filled craters with low vapor pressure form. Cyclic stress occurs when these craters or voids collapse near a metal surface. It causes surface fatigue, which contributes to the wear of the base material over time.

3. Wear Tests

The wear rate is defined as the volume loss per unit sliding distance. It is a dimensionless quantity (K) that can assess wear damage. The wear rate is defined as the body's height adjustment ratio to the relative sliding distance duration.

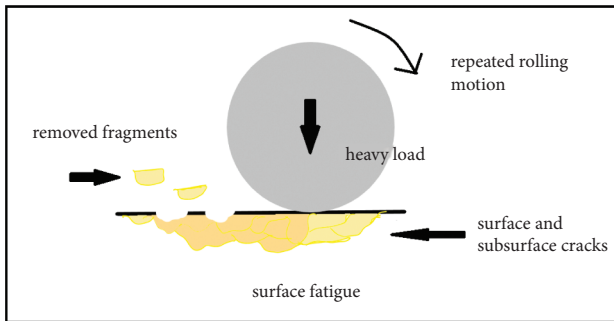


FIGURE 4: Surface fatigue.

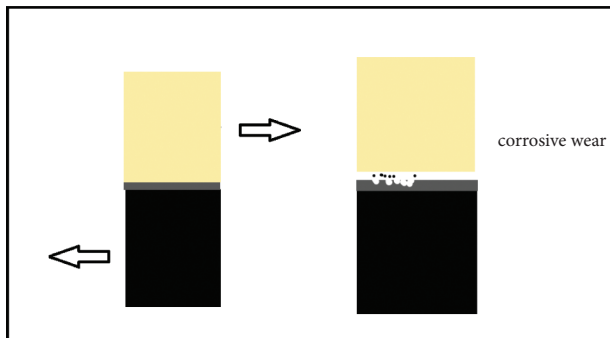


FIGURE 5: Corrosive wear.

Under normal conditions, wear progresses through three stages, the first of which is the primary stage, during which the surfaces involved adjust to one another, and the wear rate can be high or low. The second level, also known as the mid-age process, follows the first and is distinguished by a consistent wear rate. This process consumes the majority of the component's operating life. Finally, the component reaches the tertiary level, also known as the "old-age phase." The surfaces involved experience rapid wear, resulting in the component's premature failure [3–11].

Wear tests are classified as follows:

- (1) *Pin-on-Disc Wear Test*. This is one of the most common ways to test wear rates and wear resistance. It is popular due to its ability to simulate various wear modes including omnidirectional, bidirectional, unidirectional, and quasi-rotational wear. Many different materials can be tested for wear. A test of wear resistance between PTFE (polytetrafluoroethylene) and its composites [12] was done using a pin-on-disc wear test, and it was observed that as the load increased, the coefficient of friction decreased. Pure PTFE experienced maximum wear followed by PTFE with 17% GFR, PTFE with 25% bronze, and PTFE with 35% carbon which experienced minimum wear.
- (2) *Block-on-Ring Wear Test*. This is widely used to evaluate the sliding wear behavior of materials in various simulated conditions. It also helps in ranking material couples for specific tribological applications. A test of woven glass fibers is conducted on a block-on-ring wear testing machine [13], and it was

found that aramid fiber-reinforced composites are less prone to wear than simple glass fabrics. Also, weaved 300 glass fabrics displayed better wear resistance than woven 500 glass fabrics.

- (3) *Abrasion Wear Test*. This is used to test the abrasive resistance of materials such as metals, composites, ceramics, thick thermal spray, and weld overlay coatings.
- (4) *Cavitation Erosion Vibratory Test*. The surface of the test sample is immersed in liquid, and the cavitation process is induced by vibrational erosion. Ultrasonic waves consisting of alternate expansions and compressions are transmitted into the liquid, which causes erosion (material loss) of the surface of the sample. This method is used to determine the relative wear resistance of test samples to cavitation erosion. In a test between HN steel and AISI 304 steel [14], the samples' cavitation wear increased with the decrease in the pH value of the water. Also, AISI 304 steel was more resistant to wear than HN steel.
- (5) *Ball-on-Flat Wear Test*. This allows observing the wear tracks' dynamic load, friction force, and depth. Three different teeth from three different young males were tested using this apparatus [15], and it was observed that, for all the three teeth, three different wear scars were observed. The enamel layer displayed better wear resistance and had a lower friction coefficient than the dentin region.

4. Wear Testing Case Studies

Tables 1 to 5 discuss various case studies that involve various wear tests, briefly discussing the test and the implementations or additions in the metal workpiece chosen along with the observed outcomes.

5. Computational and Artificial Intelligence Models to Detect Wear Behavior

Artificial neural networks are a subset of AI widely used in mechanical engineering. ANNs are modelled after the biological neural system like an animal brain and are made up of neurons linked to each other that perform complex computations in the same way that the brain does. Dr. Robert Hecht-Nielson defined ANNs as "a *computing system composed of several simple, highly interconnected processing elements that process information through their dynamic state response to external inputs.*" The networks are widely applicable in solving classification and optimization problems, predictions, pattern recognition, etc. Because ANNs are adaptable, they can imitate linear and nonlinear relationships since the data are divided into various layers, making them well generalizable. These are trained using the datasets defined for training and then further used to predict the output values with the help of different algorithms (Figure 6) [4, 5].

TABLE 1: Comparison of materials with the pin-on-disc wear test and the results observed.

Materials used	Tests performed	Results observed	Ref.
The unreinforced portion was made of aluminum alloy (Al-2014). Various SiC particles were added to the Al alloy as a reinforcing substance.	Pin-on-disc wear test	With the increase in grain size, weight loss was observed to increase. It was discovered that composites with larger particle sizes had better wear resistance. Due to the relative motion of AZ91D and stainless steel, frictional heat is generated, which affects the rate of wear.	[16]
AZ91D alloy	Pin-on-disc	The acetal gear pair has a higher wear rate than the nylon gear pair. Each acetal gear pair has a sliding speed threshold above which the wear rate dramatically increases.	[17]
1. Nylon gears 2. Acetal gear pairs	Pin-on-disc	The wear rate of the base alloy with no reinforcements was the highest, while the composites had the lowest wear rate. Because of a solid particle-matrix interface, the alloy reinforced with SiC particles had a low wear rate, whereas the alloy reinforced with SiC fibers had a higher wear rate due to a weak fiber-matrix interface.	[18]
A substrate made of BBS: LM 11 alloys was used, which was reinforced with (a) SiC particles and (b) SiC fibers for producing composites.	Pin-on-disc	A constant rate of steady-state wear was observed. POM polymer observed the highest wear out of all. It had the highest wear rate across all sliding distances.	[19]
Glass fiber-reinforced polyphenylene sulfide polymers APK polymer POM polymer UHMWPE polymer PA66 polymer 147 Al alloy matrix composite containing the following: 1. 10% B4C 2. 15% B4C 3. 20% B4C 4. 4147 Al/SiC composite	Pin-on-disc	Due to stronger SiC particle binding to the alloy matrix, Al/SiC matrix alloys outperformed AL/B4C alloys in terms of wear resistance.	[20]
Aluminum syntactic foam	Pin-on-disc	The wear rate decreased as the sliding velocity increased. Despite its porous nature, this material showed strong wear resistance.	[21]
Untreated G3500 cast iron and S0050A cast steel Treated G4TG3500 cast iron and TS0050A cast steel	Pin-on-disc	Untreated and treated cast iron outperformed untreated cast steel in wear resistance. Both EPN-treated substrates outperformed untreated substrates in terms of wear resistance.	[22]
1. AA6061 alloy 2. AA6061 + 20 vol.% Saffil 3. AA6061 + 20 vol.% SiCp 4. AA6061 + 11 vol.% Saffil + 20% SiCp 5. AA6061 + 60 vol.% SiCp	Pin-on-disc test	Weight loss was found to decrease as the volume percent of the reinforcement was increased. Wear resistance was highest in the 60 percent SiCp composite.	[23]
1. PEEK 2. PEK 3. PEKK	1. Pin-on-disc test 2. Abrasion test on rubber wheels	A linear increment in wear volume was observed with sliding distance and sliding load increase.	[24]
1. Alloy 2014 2. Alloy 2024 3. Cast alloy 201 containing Al ₂ O ₃ and SiC	Pin-on-disc	Wear resistance was higher in aluminum matrices with a high weight percent with no metallic component. SiC-containing alloys showed a substantial change. MMCs have a slightly lower wear rate than grey cast iron.	[25]
1. Grey cast iron 2. A356/25SiCp aluminum metal matrix composite	Pin-on-disc	Resistance to wear for Al-SiC MMC is reported to be more significant than that to Al; with an increase in reinforcement volume, wear resistance reportedly increased.	[26]
1. Al 2. Al + 10 SiC 3. Al + 20 SiC 4. Al + 30 SiC 5. Al + 40 SiC	Pin-on-disc	The handled specimen has shallower and thinner wear tracks than the untreated alloy.	[27]
Ti-6Al-4V alloy without thermal oxidation and Ti-6Al-4V alloy with thermal oxidation	Pin-on-disc	Al-SiC composites displayed lower resistance to wear than Al-SiC-Gr hybrid composites.	[28]
1. Al-SiC-Gr composites 2. Al-SiC composites	Pin-on-disc	The aluminum-scandium alloy outperformed the pure industrial alloy in terms of wear resistance.	[29]
Commercially available pure Al and aluminum-scandium alloy	Pin-on-disc		[30]
			[31]

TABLE 1: Continued.

Materials used	Tests performed	Results observed	Ref.
1. PEEK 2. 20 wt.% GF-PEEK 3. 30 wt.% GF-PEEK 4. 30 wt.% CF-PEEK Al-7Si alloy reinforced with the following:	Pin-on-disc	According to the pin-on-ring sliding test, PEEK has a higher wear resistance than other thermoplastics. Carbon fibers outperformed glass fibers in terms of wear resistance.	[32]
1. 0 wt.% 2. 5 wt.% 3. 10 wt.% TiB ₂	Pin-on-disc	The wear rate decreased with an increase in TiB ₂ content in the alloy.	[33]
1. Mg-9Al 2. Mg-9Al with SiC-reinforced composite	Pin-on-disc	Due to high load-bearing capacity, the composite displayed significant wear resistance.	[34]
Brushes made of copper and graphite	Wear test with a pin-on-slip ring	Under 30 kPa BSP, arc erosion wear was the dominant wear process; abrasion wear was dominant above 120 kPa BSP.	[35]
18 polymers were examined	Pin-on-disc	PA 66-PTFE, POM-PTFE, PETP-PTFE, and PEEK-PTFE may be used in dry air. PA 66, PA 66-PTFE, and POM are the best materials for use in water.	[36]

TABLE 2: Comparison of materials with the block-on-ring wear test and the results observed.

Materials used	Tests performed	Results observed	Ref.
In one experiment, the NiCrBSi castellan PE 3309 alloy was flame sprayed onto prism-shaped grey cast iron, and in another, the alloy was laser remelted.	Block-on-ring test	The laser remelted coating wore out faster. The most common wear mechanism discovered is adhesion.	[42]
The substrate is grey cast iron, and the coating material is NiCrBSi alloy powder.	Block-on-ring test	Sliding speed had little to no effect on the wear rate as observed during the sliding test. Adhesive wear was observed at the highest loads.	[43]
Al coated with a polyetheretherketone (PEEK) composite and Al coated with a polyetheretherketone/SiC (PEEK/SiC) composite	Block-on-ring test	Compared to aluminum substrates, both polymer coatings showed a substantial improvement in wear resistance. In most sliding conditions, the addition of SiC to polymer coatings improved wear resistance even further.	[44]
WC-Co cemented carbides	Block-on-ring test	As the binder content of the WC-Co alloys increased, the wear rate caused by slipping increased.	[45]

TABLE 3: Comparison of materials with abrasive wear tests and the results observed.

Materials used	Tests performed	Results observed	Ref.
By compressing commercially available jute with the polypropylene thermoplastic matrix, composites were produced. Half of the composites were incorporated with maleic anhydride-grafted polypropylene, dissolved in toluene solution. The other half was left untreated.	Abrasion experiments were carried out using an SUGA abrasion tester.	Compared to the treated jute fiber, the untreated jute fiber showed more substantial volume loss.	[46]
1. Cold-formed steel, hot rolled 2. Wear-resistant steel with a low carbon content that has been hot rolled 3. Cold-rolled martensitic wear-resistant steel 4. Wear-resistant martensitic steel that has been tempered and quenched 5. Wear-resistant steel, bainitic, hot rolled	Impact/abrasion tester with impeller tumbler	The most weight was lost in hot-rolled cold-formed steel, then by tempered and quenched wear-resistant steel.	[47]
1. Commercially pure aluminum 2. Aluminum-magnesium alloys	1. Sliding wear tests 2. Abrasive wear tests	The Mg content in the matrix increased as metal-metal wear resistance and metal-abrasive wear resistance increased.	[48]
Grey cast iron plate	Abrasion test	Wear resistance is improved with hard-facing electrodes that contain more chromium and carbon.	[49]

TABLE 3: Continued.

Materials used	Tests performed	Results observed	Ref.
WC-Co powders used were as follows: 1. 17 wt.% Co and 83 wt.% WC 2. 15 wt.% Co and 85 wt.% WC	Abrasion test	Traditional powder-sprayed coating has a lower wear rate than HVOF-sprayed WC-Co coating.	[50]
Composites used were as follows: 1. Carbon/epoxy 2. Glass/epoxy 3. Aramid/epoxy 4. Aramid/polyetheretherketone 5. Carbon/polyetheretherketone	Abrasion test	A polyetheretherketone matrix is reinforced by oriented aramid and carbon fibers parallel to the surface. The composite was stated as a low-wear composite material.	[51]
Three plasma-sprayed coatings: 1. Al ₂ O ₃ 2. Al ₂ O ₃ -13% TiO ₂ 3. Cr ₂ O ₃ (with NiCoCrAlY bond coat)	1. Dry sliding experiments with a ball on a disc 2. Test on a dry sand-steel wheel	Plasma-sprayed ceramics displayed better results than HVOF coatings in dry particle abrasion conditions. The plasma-sprayed Cr ₂ O ₃ and HVOF-coated ceramics displayed the best results in the pin-on-disc test.	[52]
Two HVOF-sprayed cermet coatings: 1. WC-17% Co 2. WC-10% Co-4% Cr			

TABLE 4: Comparison of materials with the corrosion wear test and the results observed.

Materials used	Tests performed	Results observed	Ref.
1. AISI 1045 steel with HVOF cermet coating 2. AISI 1045 steel with a hard chromium coating	Tribocorrosion tests	HVOF-coated materials outperformed hard chromium-coated steel in terms of wear resistance.	[37]

TABLE 5: Comparison of materials with other types of wear tests and the results observed.

Materials used	Tests performed	Results observed	Ref.
Epoxy resin Carbon nanotubes	Ball-on-prism tribometer	Wear resistance was improved when CNTs were combined with an EP matrix.	[38]
Cemented carbide tools	Disc turning test	The most prevalent wear mechanisms observed were built-up edge, adherent layer, and diffusion.	[39]
Nylon gears and acetal gears	Back-to-back test configuration	The wear characteristics of nylon gears vary significantly from those of acetal gears.	[40]
Ni-SiC composites	Ring-on-disc test	With the increase in the percentage of SiC, the wear resistance of the deposited layer increases.	[41]

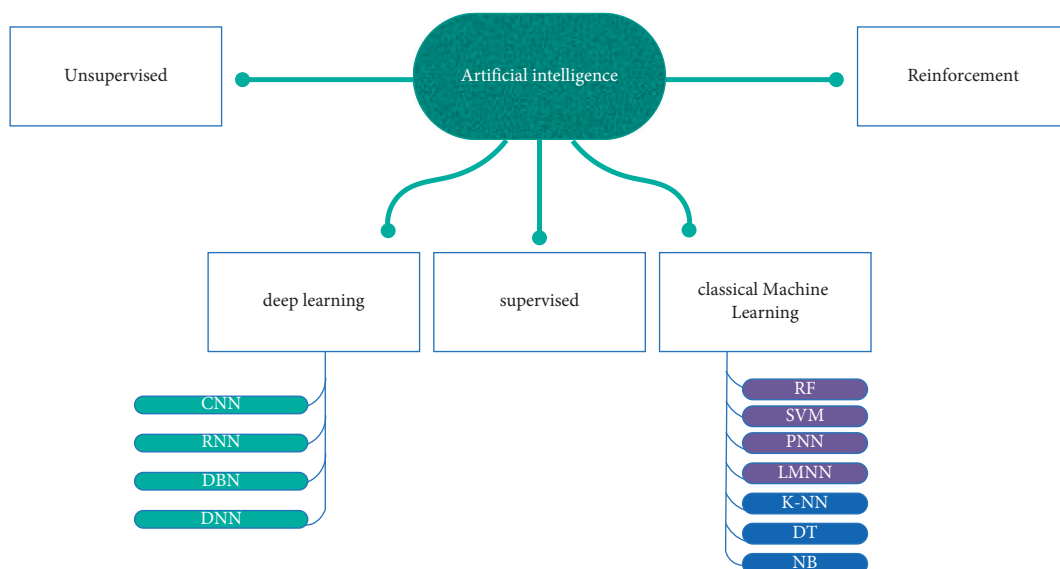


FIGURE 6: AI models: taxonomy.

TABLE 6: Algorithms used for evaluation of wear behavior in different metals.

Algorithm used	AI model taxonomy	Depth, layer sizes, training time, testing time	Dataset	Framework, core language, interface	Ref.
The backpropagation algorithm trains the weights of feedforward NNs consisting of multiple layers to predict the mass loss quantities of A390 aluminum alloy.	Supervised learning	An NN has a first layer containing three neurons and a second layer containing two neurons; overall, a two-hidden-layer network was used.	Data were normalized in the middle of [0, 1].	No data	[53]
An NN containing two hidden layers was used. The standard load, environment, and time are the three input variables. The amount of wear loss and microhardness are the two output variables. The LMA was used to train the ANN along with BP.	Supervised learning method: BP	Three layers, 3-2-2 topology	No data	No data	[54]
trainlm (network training function) was used to train a multilayer ANN. Two outputs were recorded. The LMA was applicable in adjusting the biases and weights.	Feedforward NN with BP	The ANN with three inputs and two hidden layers has the first layer containing 20 and 30 neurons. The data used for training were 70% and 15% each for validation and testing.	No data	MATLAB 2016a for the ANN Minitab 16 for visualizing the linear regression model	[55]
The NNs were diversified and tested to discover the most acceptable results possible. Thrust, cutting speed, and force were the inputs, and tool wear was the output. In contrast, the second is for predicting the surface roughness. SVR (support vector regression) was applied to solve the regression problem, and here the least square error is also used; therefore, it is known as LSSVM.	Feedforward NN using BP	NN topologies 3-5-1 and 3-4-1 were tested for tool wear, and 4-6-1 and 4-6-4-1 were tested for predicting surface roughness.	Laboratoire Génie de Production, ENIT Tarbes, France	No data	[56]
A model having a three-layer Taguchi coupled ANN was proposed. The input nodes were sliding distance, load, sliding velocity, and weight percentage. The hidden layer had seven neurons, whereas the output layer had a single neuron. The LMA was used to train this model.	LSSVM	The kernel chosen was the radial basis function.	No data	MATLAB 2013	[57]
The network consists of three layers and four PCA-declared input nodes, whereas the hidden layer has three nodes, and the output layer having a single node was best out of all the networks. The first two layers used the neural transfer function tansig, whereas the last layer used purelin.	Supervised learning	3-7-1 architecture ANN	No data	MATLAB 2013	[58]
	Supervised learning	4-3-1 architecture with the three-layer feedforward ANN	No data	A commercial Neural Network Toolbox	[59]

TABLE 6: Continued.

Algorithm used	AI model taxonomy	Depth, layer sizes, training time, testing time	Dataset	Framework, core language, interface	Ref.
Adaptive neuro-fuzzy inference system combines the “Takagi–Sugeno fuzzy inference system” and the principles of ANN.	Supervised learning	Five layers in ANFIS	No data	MATLAB	[60]
Taguchi technique has been used here. A weight-loss model to make predictions was made using regression. Nonlinear regression was used to correlate control factors and weight loss.	Supervised learning	No data	No data	Minitab 15.1	[61]
The AI algorithms used here are random forests, regression trees, MLP, and RBF.	Supervised learning: MLP, RBF, and random forests	RBF has one layer, and MLP has one hidden layer.	The experimental data were collected to provide a broad number of wear conditions and processing times while acquiring data on the power drive for a fixed machining process—the face milling of carbon-quality structural steel 45.	No data	[62]
“Kohonen’s self-organizing map” was used to evaluate the tool’s working status. Also, a triangular membership function applied neuro-fuzzy and fuzzy logic. The “centroid method of defuzzification” was used to obtain the flank wear.	Supervised learning: backpropagation NN	2-3-1 architecture	The training data for the networks were collected through experimental studies.	No data	[63]
One neuron represents each input parameter distinctively related to the coefficient of friction. The input variables include applied load, sliding velocity, sliding distance, and material type, whereas the output is the coefficient of friction. It has 4-6-4-1 architecture. An MLP model was applied here because of its feedforward nature.	Supervised learning: MLP	4-6-4-1 architecture	No data	No data	[64]
For evaluating the tool wear, a developed configuration system was applied. Also, using an expert system at different wear states helped clarify the output values of ANN.	Unsupervised learning: ART2	Number of input neurons in SOM: 15, and number of neurons in an SOM layer: 36	No data	No data	[65]
The network used in this study was a generalized feedforward network. Input parameters were sliding time, sliding speed, load, and Al-Si%, whereas the output parameter was specific wear rate. The network consisted of three hidden layers with 16, 8, and 5 neurons.	Supervised learning	4-11-5-1 architecture and two hidden layers with four inputs and one output layer were applied.	No data	No data	[66]
The first two layers used the TanhAxon function, whereas the last layer applied the BiasAxon function.					

TABLE 6: Continued.

Algorithm used	AI model taxonomy	Depth, layer sizes, training time, testing time	Dataset	Framework, core language, interface	Ref.
The LMA along with BP was applied in this study. Load and speed are the two nodes of the input layer, whereas the friction and mass loss coefficient are the two nodes of the output layer. The minimal fault was observed in the output due to ten neurons in the hidden layer.	Supervised learning	Two output and ten hidden neurons	No data	MATLAB	[67]
The proposed reduction model here is a combination of POD and RBF.	Supervised learning	The network consists of two layers, one with RBF neurons and the other with output neurons.	No data	MATLAB	[68]
The ANN was trained with the Levenberg–Marquardt algorithm (LMA), Bayesian regulation (BR), resilient backpropagation (RP), scaled conjugate gradient (SCG), and gradient descent (GD).	Supervised learning	Five distinct training algorithms were used, along with eighteen different architectures. The Bayesian algorithm trained in a two-layered neural network has reached the best results (26 10 5 1).	Training data were obtained by 360 randomly distributed data collected from testing of four friction materials. Training data were acquired by testing eight different friction materials, only predicting fade performance.	No data	[69]
The ANN and Sugeno FIS have been applied, and BP having 4-3-1 architecture and LMA is adopted here.	Supervised learning: backpropagation	The network has 4-3-1 architecture and one hidden layer.	No data	MATLAB R2015a using NN Toolbox	[70]
FZM and ANN, along with a neuro-fuzzy ANFIS, are adopted here.	Supervised learning: backpropagation for ANN Unsupervised learning for fuzzy c-means clustering	The ANN having 4-3-1 architecture and ninety-cluster C-mean clustering gave the best performance.	No data	No data	[71]
The Elman-inspired RNN was applied. The sensor uses the relationship between the variables to be measured and the power consumption.	Bayesian regularization	The best model HU55 implies five hidden units and a delay of 5.	A Training and Test Data Set (TTDS) is generated with a specific combination of the grinding experiments collected.	MATLAB	[72]
RF, MLP, RBF, etc., were used in this study to predict surface roughness and mass loss.	Supervised learning: regression trees, MLP BP	A network having a three-layer architecture and a hidden layer consisting of RBF was used.	No data	No data	[73]
Output, i.e., tool wear, is predicted with the help of residual errors as the basis of decision-making.	Supervised learning: MLP	MLP has 6-12-1 architecture, and one hidden layer was used here.	No data	MATLAB	[74]
Volume loss is predicted using LR, SVM, ANN, and other extreme learning methods.	Supervised learning: ANN, SVR, and LR	The ANN has a 3-4-1 architecture and a quadratic function as the SVR kernel, whereas ELM used here is a feedforward NN having a single hidden layer.	Experimentally obtained data	MATLAB	[75]

TABLE 6: Continued.

Algorithm used	AI model taxonomy	Depth, layer sizes, training time, testing time	Dataset	Framework, core language, interface	Ref.
Supervised learning methods such as SVR, RF regression, decision tree regression, GBR, GPR, MLP, and KNN are used.	Supervised learning	SVR uses an RBF for the kernel. MLP having five hidden layers and ten neurons in each layer with ReLU activation was used here.	Collected from 13 references of 316L SS parts processed by SLM	Python TensorFlow, scikit-learn, Google Colab	[76]
The ANN with BP is applied along with ANOVA to decide the potential parameters to predict the specific wear rate reduction.	Supervised learning	The ANN has the 2:5:1 architecture with sigmoid activation.	No data	Python, Minitab 19	[77]
Analysis of the erosion process is done using the ANN model along with LMA.	Supervised learning	The network having three layers and 2-6-3 architecture is used here.	No data	MATLAB 2017a Neural Network Toolbox	[78]
ANN and RSM models were compared based on their predictive capacity of wear behavior of fabricated composites.	Supervised learning	Three inputs, ten hidden layers, and two outputs	No data	MATLAB	[79]

TABLE 7: Advantages and disadvantages of the above-discussed algorithms (Table 6) used to evaluate wear behavior in different metals.

Advantages	Disadvantages	Ref.
NNs are quite enduring as the parameter (weight) values are changed according to the performance. The modifications are made according to an ML algorithm called gradient descent (GD).	Other algorithms like SVM in [56] could be implemented and compared for better performance and results. For example, the LMA (Levenberg–Marquardt algorithm) could improve the model instead of GD.	[53]
The model was concluded to be excellent and fast because of the little prediction time, and the results of the ANN model, along with the experimental study, indicated the same. Also, the LMA was faster than GD or GN.	The LMA gives us only the local optimum instead of the global optimum.	[54]
The experiment helped perceive the most influential factors affecting the friction coefficient and the wear rate. Therefore, the ANN is very much capable of predicting the same.	Because the derivatives of the flat functions do not exist after a certain point in time, the algorithm might be a failure.	[54]
NNs can take in linear and nonlinear relationships, generating and performing well to show good results.	The LMA might not be a potential choice if the beginning point does not have the right quality, i.e., distant from the actual required values.	[55]
LSSVM could eliminate local minima. Also, comparing the relative error of RSM and LSSVM, the graph depicts LSSVM as a suitable model since it has fewer relative errors.	Sigmoid (the activation function) was not zero-centered that could give undesired results and implications during the implementation of GD. An alternative for it could be tanh, and where priority is speed, ReLU would be suitable.	[56]
To obtain an optimal value of the input parameter and achieve an output value with the minor target, Taguchi coupled ANN was applied.	SVM underperforms if the number of characteristics for a data point exceeds the number of training data samples. Therefore, a considerable amount of data are required to be enforced.	[57]
The ANN was better than a statistical approach since it has three times lower relative mean error and higher stability for all studied conditions.	The effects of a parameter on the resultant value were not precise. Also, the method did not provide any absolute results; therefore, it was stated unsuitable for a constantly changing process.	[58]
The aim behind ANFIS is to connect inputs and outputs accurately. It could help set up a model with uncertainties and composite data distribution.	A model without units makes the equations incomprehensible physically; therefore, it is necessary to include units to make sense in the world.	[59]
To determine parameters having minimum variations, Taguchi methods were helpful. Also, ANOVA was used to check the quality of features affected by design parameters.	The limitations of ANFIS are the computational expense, and it is hard to compute large input values. Therefore, it cannot be used in a big data paradigm.	[60]
RF showed the highest precision. Due to its ability to get tuned and give visual information, RF can be directly used by product engineers.	The effects of a parameter on the resultant value were not precise. Also, the method did not provide any absolute results; therefore, it was stated unsuitable for a constantly changing process.	[61]
To improve user-friendliness, linguistic rules were applied. Also, for fuzzy logic, they act as an advantage.	The RF creates many trees and needs a lot of computational power and colossal training time.	[62]
	Overfitting of noisy data may lead to unfavorable outputs.	
	To achieve a stable mapping with the help of Kohonen’s SOM, the nearby data point needs to behave similarly.	[63]

TABLE 7: Continued.

Advantages	Disadvantages	Ref.
The ANN aids in estimating the coefficient of friction for parameter values more significant than those included in POD experiments.	Increasing the total number of parameters in an MLP might lead to more time. It is inefficient as such high dimensions might be redundant.	[64]
An ANN and expert systems were used to find the worn-out tools. A blend of inference results and complex sensor outputs helped achieve a positive result.	Expert systems collapse without a proper output from the ANN; therefore, they will face issues classifying the tool's wear.	[65]
GFs usually take in more compound, nonlinear, and unpredictable relationships since their connections can skip several layers.	A network of this kind could overfit due to its inability to deduce the latest data when applied to simple tasks.	[66]
ANN's characteristics like adaptability and fault tolerance are beneficial here.	The beginning point is far off the desired value; the LMA might not perform well here.	[67]
The unknown parameters can be found through this technique if the outputs are already known.	Massive space for inputs is required when using RBF though it is not favorable to waste inputs while having other essential tasks.	[68]
Less period is required for training the Bayes, and its application is effortless.	The nature of the attributes is presumed to be mutually independent in the Bayesian algorithm, but that seems impossible as the predictors cannot be fully independent.	[69]
Results were in order with the experimental values; therefore, the neuro-fuzzy approach is good.	Sugeno FIS provided no output membership function, and chances of loss of interpretability are high.	[70]
A framework based on the Takagi–Sugeno neuro-fuzzy network has proven to be the best of both worlds.	Massive inputs and computational expenses are some of the limitations of ANFIS. Therefore, it is not applicable for a “big data paradigm.”	[71]
The RNN can mimic the dynamic nature of the problem here as the old network values are reused, in turn, giving the ANN memory.	There can be problems with the gradient not converging. It is a complex task while working with tanh or ReLU activation functions.	[72]
RF is concluded to be best for industry purposes as no parameter tuning was required for it. Also, its predictions are equally good as MLPs.	The RF creates several trees; therefore, it requires more computational power and more training time.	[73]
This model practices a high-powered working nature, whereas a supervision system cannot.	Chances of noisy overfitting data having unfavorable outputs as results are there.	[73]
An R2 error value of 0.989 was obtained using the ELM method, and a reduced number of tests, testing time, and cost were also observed here.	A neuro-FIS might be applicable in such a dynamic environment.	[74]
GBR was concluded as the best out of the seven ML algorithms compared here since it resulted in the slightest standard deviation and good accuracy.	More training cases could lead to the loss of the essence of the problem as the ELM consists of only one hidden layer. This was not observed here since the number of cases is only 40.	[75]
Minimum error artificial data were generated for processing, and the method used here is flexible and considered best for evaluating the tribo-parameters.	KNN, STR, and GPR will not be recommended as they are considered the worst-performing algorithms here.	[76]
The ANN investigated the impact on the APS process parameters well.	The work is limited to the general behavior of distinct reinforcement particles due to the variable metallurgical properties.	[77]
A regression coefficient value of 0.99996 using the ANN was the best of all the other proposed models.	Future work includes the optimum coating properties dependent on the APS process parameters.	[78]
	Different algorithms could be used for training the ANN along with GBR and SVR, and it can be used to compare the results.	[79]

- (1) ANNs typically have three main layers. Input layer: The layer to which input data and patterns are fed is always a single input layer.
- (2) Hidden layers: There could be several of these layers. Behind the scenes, processing occurs, and the output is calculated based on “weights,” which determine the significance of a specific characteristic. These layers also remove inessential data from the input data before sending them to the hidden layer, next in line for processing.
- (3) The endmost hidden layer is linked to the output layer, which provides the final output value(s).

The center of NNs is backpropagation. It is an algorithm through which the neural network corrects itself with each iteration that relies on weights.

6. Summary and Conclusions

The research works discussed briefly in this review propose various systems for supervising the machining process, tool wear monitoring, determination of wear state for a tool, and many more. Significant research has been done involving ANNs with the LVM (as shown in Tables 6 and 7) algorithm training the models, resulting in highly generalized and fault-tolerant models; however, LVM can only provide a local optimum and may not respond to flat functions, producing unwanted results, and the starting point is way far from the optimal.

Some studies consider the ANFIS, adaptive neuro-fuzzy interface system, method that combines ANN and fluidic logic, specifically the “Takagi–Sugeno fuzzy interference system,” which can capture neural networks fumigating logic

in one. However, this model may not perform well for many inputs, i.e., this model fails in a big data paradigm. The surface roughness and wear were predicted using RNNs, i.e., ANNs having memory; hence, they are more suitable for a constantly developing environment of such wear behavior of tools. Surface wear was detected using random forests and multilayer perceptrons based on surface isotropy levels. Random forests are superior because MLPs require parameter tuning, and their output is nearly identical to that of RFs. These methods for various processes are also discussed in some research that encompasses most of the approaches [80–92].

6.1. Accuracies Achieved in Recent Research Works. Using a two-hidden-layer neural network, Kumar and Singh [53] obtained a normalized standard error of 0.00085. At the same time, Çetinel et al. [54], who also used a two-hidden-layer network but with the addition of the Levenberg–Marquardt algorithm, found an average error of 2.461% for wear (in micrometers) and 0.245% error for microhardness (in HV). A least square support vector machine to predict wear behavior in [56] yielded an average of 1.2 percent better results on 52 runs than the RSM model. Kolodziejczyk [58] used PCA preprocessing and the LVM algorithm to achieve a mean relative error of 1.8 percent, three times lower than that in previous studies. A multilayer perceptron model was used in [64], which yielded 0.0186 and 0.0180 training and testing residual errors, respectively. The SOM model had a higher correlation coefficient than the ART2 model in [65], with 0.964 and 0.946 for the training and test sets. The ANN was combined with the Taguchi method in [55], and a 99.5 percent confidence level was observed between predicted and actual wear rates and coefficients of friction. In [93], the ANN with one hidden layer had a more significant sum of squares error (SSE) of 0.025 and 0.25 for training and testing, respectively, whereas the ANN with two hidden layers had 0.008 and 0.46 SSEs for training and testing. As a result of the lower SSE, the two-hidden-layer networks were chosen, with an RMSE of 2.64 percent on average. The ANFIS models—sigmoidal, triangular, Gaussian, and bell-shaped MFs—were used [59]. The most accurate model was sigmoidal MF, which had a regression coefficient of 0.96775. RFs and MLPs were used in [62], with RFs having a better accuracy of 33 to 44 percent and an error of 0.2457 micrometers than the MLP's 0.4139. An ANFIS was used for various membership functions [70]. The RMSE was in the order of E-11, which was 0.557 for the ANN. The Sugeno-type ANFIS model had the best correlation coefficient of 97.74 percent with gbellmf membership. Nagaraj and Gopalakrishnan [66] reported an MSE of 0.0904 and an MAE of 0.1257. In [73], various ML techniques model various parameters, with MLPs better in 3/4 of them and RFs taking one of the parameters. MLPs were found to have a 52 percent accuracy rate. The ANFISs appear to have the least amount of error.

6.2. Open Issues. Multiple systems have been proposed in recent research to address the supervision process in machining, tool wear monitoring, tool wear detection, and so

on. More researchers use ANNs with the LVM algorithm to train fault-tolerant and well-generalized models, but the LVM only provides a local optimum and may not work for flat functions. If the starting point is too far from the optimal, it may also produce undesirable results. The ANFIS, adaptive neuro-fuzzy interface system, is a combination of ANN and fuzzy logic used in a few papers, specifically the Takagi–Sugeno fuzzy interference system, which can capture the essence of both neural nets and fuzzy logic in one [94–102]. However, this model may not work well for many inputs, i.e., this model fails in a big data paradigm. RNNs, which are technically ANNs with memory and thus more suited for such ever-changing dynamic environments as tool wear, were also used to predict wear and surface roughness [103–106]. Surface wear was also predicted using random forests and multilayer perceptrons and surface isotropy levels. MLPs require parameter tuning, and their output is nearly identical to that of RFs, so random forests are preferable. These various processes are also discussed in [107], which encompasses most approaches.

6.3. Future Directions. Wear analysis using artificial intelligence is a relatively new concept. Formal result: Accordingly, it was discovered that there is less work on AI than aluminum (e.g., FGP grey-coated or NiCrBSi-coated aluminum) writable composites (e.g., polymer-reinforced glass), which indicates that it is to be expected since less work has been done on AI (e.g., plastic/FGP-NiCr alloyed glass) to grasp fully [80, 108]. Further study is required to understand the full capabilities of using AI. This state-of-the-art technology for analyzing artificial neural networks is now being utilized for efficient and economical wear-resistant materials. Tool wear is one of the most common aspects of the machining process that needs to be analyzed. Research can be done on the tool metal's wear behavior in the future, and the metal can be modified and tested for wear. New research opportunities can be found to find an ideal metal for machining processes. Artificial neural networks for wear analysis can help identify the most efficient coating materials for various substrates to increase the substrate's wear resistance with accurate predictions, which is inefficient and time-consuming when identified using traditional methods. Artificial intelligence is currently limited to analyzing wear for various materials used in manufacturing and production. Still, the main benefit of using AI is studying a wide range of data and making accurate predictions. More experimentation is needed to make the most of this technology, which will allow industries to predict the time and type of wear that will occur on a material ahead of time, allowing them to continue operating without interruption [108–114].

Abbreviation

ANN:	Artificial neural network
NN:	Neural network
ML:	Machine learning
GD:	Gradient descent
LMA:	Levenberg–Marquardt algorithm

BP: Backpropagation
 GN: Gaussian network
 SVR: Support vector regression
 LSSVM: Least square support vector machine
 RSM: Response surface methodology
 RBF: Radial basis function
 MLP: Multilayer perceptron
 SOM: Self-organizing map
 GF: Generalized feedforward
 POD: Proper orthogonal decomposition
 BR: Bayesian regulation
 RP: Resilient backpropagation
 SCG: Scaled conjugate gradient
 FIS: Fuzzy inference system
 FZM: Fuzzy clustering method
 LR: Linear regression
 ELM: Extreme learning method
 RF: Random forest
 GBR: Gradient boosting regression
 GPR: Gaussian process regression.

Conflicts of Interest

The authors declare no conflicts of interest.

Authors' Contributions

Senthil Kumaran Selvaraj and Aditya Raj have Contributed Equally AR and SKS conceptualized the research idea and ran the software. SKS performed the methodology, validated the data, and administered the project. AR, MD, UC, IS, and CK were involved in formal analysis and wrote the original draft. AR, MD, and UC investigated the data and obtained the resources. AR, MD, UC, and IS curated the data. UC and CK visualized the data and reviewed and edited the paper. SKS and UC supervised the study. All the authors have read and agreed to the published version of the manuscript.

References

- [1] "Standard terminology relating to wear and erosion," *Annual Book of Standards*, vol. 03.02, pp. 243–250, 1987.
- [2] G. W. Stachowiak and A. W. Batchelor, *Engineering Tribology*, Elsevier Applied Science, Amsterdam, Netherland, 2014.
- [3] F. Kara, M. Karabatak, M. Ayyıldız, and E. Nas, "Effect of machinability, microstructure and hardness of deep cryogenic treatment in hard turning of AISI D2 steel with ceramic cutting," *Journal of Materials Research and Technology*, vol. 9, no. 1, pp. 969–983, 2020.
- [4] R. M. C. Karthik, R. L. Malghan, F. Kara, A. Shettigar, S. S. Rao, and M. A. Herbert, "Influence of support vector regression (SVR) on cryogenic face milling," *Advances in Materials Science and Engineering*, vol. 2021, Article ID 9984369, 18 pages, 2021.
- [5] A. Eser, E. A. Ayyıldız, M. Ayyıldız, and F. Kara, "Artificial intelligence-based surface roughness estimation modelling for milling of AA6061 alloy," *Advances in Materials Science and Engineering*, vol. 2021, Article ID 5576600, 10 pages, 2021.
- [6] P. Ganeshan, S. S. Kumaran, K. Raja, and D. Venkateswarlu, "An investigation of mechanical properties of madar fiber reinforced polyester composites for various fiber length and fiber content," *Materials Research Express*, vol. 6, 2019.
- [7] S. Kannan, S. S. Kumaran, and L. A. Kumaraswamidhas, "Optimization of friction welding by taguchi and ANOVA method on commercial aluminium tube to Al 2025 tube plate with backing block using an external tool," *Journal of Mechanical Science and Technology*, vol. 30, pp. 2225–2235, 2016.
- [8] S. K. Senthil, S. Muthukumaran, and C. R. Chandrasekhar, "Effect of tube preparations on joint strength in friction welding of tube-to-tube plate using an external tool process," *Experimental Techniques*, vol. 37, pp. 24–32, 2013.
- [9] V. V. Kumar and S. S. Kumaran, "Friction material composite: types of brake friction material formulations and effects of various ingredients on brake performance-a review," *Materials Research Express*, vol. 6, 2019.
- [10] S. K. Senthil, S. Muthukumaran, D. Venkateswarlu, G. K. Balaji, and S. Vinodh, "Eco-friendly aspects associated with friction welding of tube-to-tube plate using an external tool process," *Int J Sustain Eng*, vol. 5, pp. 120–127, 2012.
- [11] S. K. Senthil and A. D. Daniel, "Friction welding joints of SA 213 tube to SA 387 tube plate boiler grade materials by using clearance and interference fit method," *Materials Today Proceedings*, vol. 5, pp. 8557–8566, 2018.
- [12] H. Unal, A. Mimaroglu, U. Kadioglu, and H. Ekiz, "Sliding friction and wear behaviour of polytetrafluoroethylene and its composites under dry conditions," *Materials & Design*, vol. 25, no. 3, pp. 239–245, 2004.
- [13] H. Pihtili and N. Tosun, "Effect of load and speed on the wear behavior of woven glass fabrics and aramid fiber-reinforced composites," *Wear*, vol. 252, no. 11–12, pp. 979–984, 2002.
- [14] G. Bregliozzi, A. Di Schino, S. U. Ahmed, J. M. Kenny, and H. Haefke, "Cavitation wear behavior of austenitic stainless steels with different grain sizes," *Wear*, vol. 258, no. 1–4, pp. 503–510, 2005.
- [15] J. Zheng, Z. R. Zhou, J. Zhang, H. Li, and H. Y. Yu, "On the friction and wear behavior of human tooth enamel and dentin," *Wear*, vol. 255, no. 7–12, pp. 967–974, 2003.
- [16] Y. Şahin, "Abrasive wear behavior of SiC/2014 aluminium composite," *Tribology International*, vol. 43, no. 5–6, pp. 939–943, 2010.
- [17] N. N. Aung, W. Zhou, and L. E. Lim, "Wear behavior of AZ91D alloy at low sliding speeds," *Wear*, vol. 265, no. 5–6, pp. 780–786, 2008.
- [18] A. R. Breeds, S. N. Kukureka, K. Mao, D. Walton, and C. J. Hooke, "Wear behaviour of acetal gear pairs," *Wear*, vol. 166, no. 1, pp. 85–91, 1993.
- [19] O. P. Modi, B. K. Prasad, A. H. Yegneswaran, and M. L. Vaidya, "Dry sliding wear behaviour of squeeze cast aluminium alloy-silicon carbide composites," *Materials Science and Engineering: A*, vol. 151, no. 2, pp. 235–245, 1992.
- [20] H. Unal, U. Sen, and A. Mimaroglu, "Abrasive wear behaviour of polymeric materials," *Materials & Design*, vol. 26, no. 8, pp. 705–710, 2005.
- [21] R. Ipek, "Adhesive wear behaviour of B4C and SiC reinforced 4147 Al matrix composites (Al/B4C-Al/SiC)," *Journal of Materials Processing Technology*, vol. 162–163, pp. 71–75, 2005.
- [22] D. P. Mondal, S. Das, and N. Jha, "Dry sliding wear behaviour of aluminum syntactic foam," *Materials & Design*, vol. 30, no. 7, pp. 2563–2568, 2009.
- [23] X. Nie, L. Wang, Z. C. Yao, L. Zhang, and F. Cheng, "Sliding wear behavior of electrolytic plasma nitrided cast iron and steel," *Surface and Coatings Technology*, vol. 200, no. 5–6, pp. 1745–1750, 2005.

- [24] A. B. Gurcan and T. N. Baker, "Wear behavior of AA6061 aluminium alloy and its composites," *Wear*, vol. 188, no. 1-2, pp. 185-191, 1995.
- [25] A. P. Harsha and U. S. Tewari, "Two-body and three-body abrasive wear behaviour of polyaryletherketone composites," *Polymer Testing*, vol. 22, no. 4, pp. 403-418, 2003.
- [26] F. M. Hosking, F. F. Portillo, R. Wunderlin, and R. Mehrabian, "Composites of aluminium alloys: fabrication and wear behaviour," *Journal of Materials Science*, vol. 17, no. 2, pp. 477-498, 1982.
- [27] N. Natarajan, S. Vijayarangan, and I. Rajendran, "Wear behavior of A356/25SiCp aluminium matrix composites sliding against automobile friction material," *Wear*, vol. 261, no. 7-8, pp. 812-822, 2006.
- [28] B. Venkataraman and G. Sundararajan, "The sliding wear behaviour of AlSiC particulate composites-I. Macro-behaviour," *Acta Materialia*, vol. 44, no. 2, pp. 451-460, 1996.
- [29] H. Güleriyüz and H. Çimenoglu, "Effect of thermal oxidation on corrosion and corrosion-wear behavior of a Ti-6Al-4V alloy," *Biomaterials*, vol. 25, no. 16, pp. 3325-3333, 2004.
- [30] S. Suresha and B. K. Sridhara, "Effect of addition of graphite particulates on the wear behaviour in aluminium-silicon carbide-graphite composites," *Materials & Design*, vol. 31, no. 4, pp. 1804-1812, 2010.
- [31] K. Venkateswarlu, L. C. Pathak, A. K. Ray et al., "Micro-structure, tensile strength and wear behaviour of Al-Sc alloy," *Materials Science and Engineering: A*, vol. 383, no. 2, pp. 374-380, 2004.
- [32] H. Voss and K. Friedrich, "On the wear behaviour of short-fibre-reinforced peek composites," *Wear*, vol. 116, no. 1, pp. 1-18, 1987.
- [33] S. Kumar, M. Chakraborty, V. S. Sarma, and B. S. Murty, "Tensile and wear behavior of in situ Al-7Si/TiB₂ particulate composites," *Wear*, vol. 265, no. 1-2, pp. 134-142, 2008.
- [34] C. Y. H. Lim, S. C. Lim, and M. Gupta, "Wear behavior of SiCp-reinforced magnesium matrix composites," *Wear*, vol. 255, no. 1-6, pp. 629-637, 2003.
- [35] I. Yasar, A. Canakci, and F. Arslan, "The effect of brush spring pressure on the wear behaviour of copper-graphite brushes with electrical current," *Tribology International*, vol. 40, no. 9, pp. 1381-1386, 2007.
- [36] J. W. M. Mens and A. W. J. D. Gee, "Friction and wear behavior of 18 polymers in contact with steel in environments of air and water," *Wear*, vol. 149, no. 1-2, pp. 255-268, 1991.
- [37] L. Fedrizzi, S. Rossi, R. Cristel, and P. L. Bonora, "Corrosion and wear behavior of HVOF cermet coatings used to replace hard chromium," *Electrochimica Acta*, vol. 49, no. 17-18, pp. 2803-2814, 2004.
- [38] O. Jacobs, W. Xu, B. Schädel, and W. Wu, "Wear behaviour of carbon nanotube reinforced epoxy resin composites," *Tribology Letters*, vol. 23, no. 1, pp. 65-75, 2006.
- [39] G. List, M. Nouari, D. Géhin et al., "Wear behavior of cemented carbide tools in dry machining of aluminium alloy," *Wear*, vol. 259, no. 7-12, pp. 1177-1189, 2005.
- [40] K. Mao, W. Li, C. J. Hooke, and D. Walton, "Friction and wear behavior of acetal and nylon gears," *Wear*, vol. 267, no. 1-4, pp. 639-645, 2009.
- [41] K. H. Hou, M. D. Ger, L. M. Wang, and S. T. Ke, "The wear behavior of electro-codeposited Ni-SiC composites," *Wear*, vol. 253, no. 9-10, pp. 994-1003, 2002.
- [42] R. Gonzalez, M. Cadenas, R. Fernandez, J. L. Cortizo, and E. Rodriguez, "Wear behavior of flame sprayed NiCrBSi coating remelted by flame or by laser," *Wear*, vol. 262, no. 3-4, pp. 301-307, 2007.
- [43] E. Fernández, M. Cadenas, R. González, C. Navas, R. Fernández, and J. D. Damborenea, "Wear behavior of laser clad NiCrBSi coating," *Wear*, vol. 259, no. 7-12, pp. 870-875, 2005.
- [44] G. Zhang, H. Liao, H. Li, C. Mateus, J.-M. Bordes, and C. Coddet, "On dry sliding friction and wear behaviour of PEEK and PEEK/SiC-composite coatings," *Wear*, vol. 260, no. 6, pp. 594-600, 2006.
- [45] J. Pirso, S. Letunoviš, and M. Viljus, "Friction and wear behavior of cemented carbides," *Wear*, vol. 257, no. 3-4, pp. 257-265, 2004.
- [46] N. Chand and U. K. Dwivedi, "Effect of coupling agent on abrasive wear behaviour of chopped jute fibre-reinforced polypropylene composites," *Wear*, vol. 261, no. 10, pp. 1057-1063, 2006.
- [47] A. Sundström, J. Rendón, and M. Olsson, "Wear behavior of some low alloyed steels under combined impact/abrasion contact conditions," *Wear*, vol. 250, no. 1-12, pp. 744-754, 2001.
- [48] A. Hayrettin, K. Tolga, C. Ercan, and C. Huseyin, "Wear behavior of Al/(Al₂O₃p/SiCp) hybrid composites," *Tribology International*, vol. 39, pp. 213-220, 2006.
- [49] S. Chatterjee and T. K. Pal, "Wear behavior of hardfacing deposits on cast iron," *Wear*, vol. 255, no. 1-6, pp. 417-425, 2003.
- [50] D. A. Stewart, P. H. Shipway, and D. G. McCartney, "Abrasive wear behaviour of conventional and nano-composite HVOF-sprayed WC-Co coatings," *Wear*, vol. 225-229, pp. 789-798, 1999.
- [51] M. Cirino, R. B. Pipes, and K. Friedrich, "The abrasive wear behaviour of continuous fibre polymer composites," *Journal of Materials Science*, vol. 22, no. 7, pp. 2481-2492, 1987.
- [52] G. Bolelli, V. Cannillo, L. Lusvarghi, and T. Manfredini, "Wear behavior of thermally sprayed ceramic oxide coatings," *Wear*, vol. 261, no. 11-12, pp. 1298-1315, 2006.
- [53] A. Kumar and D. Singh, "Artificial neural network-based wear loss prediction for A390 aluminium alloy," *Journal of Theoretical and Applied Information Technology*, vol. 4, no. 10, 2008.
- [54] H. Çetinel, H. Öztürk, E. Çelik, and B. Karlık, "Artificial neural network-based prediction technique for wear loss quantities in Mo coatings," *Wear*, vol. 261, no. 10, pp. 1064-1068, 2006.
- [55] B. Stojanović, A. Vencl, I. Bobić, S. Miladinović, and J. Skerlić, "Experimental optimisation of the tribological behaviour of Al/SiC/Gr hybrid composites based on Taguchi's method and artificial neural network," *Journal of the Brazilian Society of Mechanical Sciences and Engineering*, vol. 40, no. 6, 2018.
- [56] S. B. Mishra, R. Pattnaik, and S. S. Mahapatra, "Parametric analysis of wear behaviour on fused deposition modelling build parts," *International Journal of Productivity and Quality Management*, vol. 21, no. 3, pp. 375-391, 2017.
- [57] V. Kavimani and K. S. Prakash, "Tribological behaviour predictions of r-GO reinforced Mg composite using ANN coupled Taguchi approach," *Journal of Physics and Chemistry of Solids*, vol. 110, pp. 409-419, 2017.
- [58] T. Kolodziejczyk, R. Toscano, S. Fouvry, and G. E. Morales, "Artificial intelligence as efficient technique for ball bearing fretting wear damage prediction," *Wear*, vol. 268, no. 1-2, pp. 309-315, 2010.
- [59] M. Marani, M. Zeinali, J. Kouam, V. Songmene, and C. K. Mechefske, "Prediction of cutting tool wear during a turning process using artificial intelligence techniques,"

- International Journal of Advanced Manufacturing Technology*, vol. 111, no. 1-2, pp. 505–515, 2020.
- [60] L. Monostori, “AI and machine learning techniques for managing complexity, changes and uncertainties in manufacturing,” *Engineering Applications of Artificial Intelligence*, vol. 16, no. 4, pp. 277–291, 2003.
- [61] P. Padmanabhan, A. Arulbrittoraj, R. Srinivasan, and G. Ebenezer, “Study the influence of case hardening and sliding wear parameters on carburised AISI 1211 steel,” *International Journal of Surface Science and Engineering*, vol. 10, no. 5, p. 415, 2016.
- [62] D. Y. Pimenov, A. Bustillo, and T. Mikolajczyk, “Artificial intelligence for automatic prediction of required surface roughness by monitoring wear on face mill teeth,” *Journal of Intelligent Manufacturing*, vol. 29, no. 5, pp. 1045–1061, 2017.
- [63] C. S. Rao and R. R. Srikant, “Tool wear monitoring-an intelligent approach,” *Proceedings of the Institution of Mechanical Engineers - Part B: Journal of Engineering Manufacture*, vol. 218, no. 8, pp. 905–912, 2004.
- [64] T. Sahraoui, S. Guessasma, N. E. Fenineche, G. Montavon, and C. Coddet, “Friction and wear behaviour prediction of HVOF coatings and electroplated hard chromium using neural computation,” *Materials Letters*, vol. 58, no. 5, pp. 654–660, 2004.
- [65] R. G. Silva, S. J. Wilcox, and R. L. Reuben, “Development of a system for monitoring tool wear using artificial intelligence techniques,” *Proceedings of the Institution of Mechanical Engineers - Part B: Journal of Engineering Manufacture*, vol. 220, no. 8, pp. 1333–1346, 2006.
- [66] A. Nagaraj and S. Gopalakrishnan, “Modelling wear behavior of aluminium-silicon alloys using generalized feed forward neural network,” *Tierärztliche Praxis*, vol. 40, 2020.
- [67] D. Vijay and T. K. Kandavel, “Application of artificial neural network on wear properties of sinter-forged Fe-C-Mo low alloy steel,” *International Journal of Advanced Intelligence Paradigms*, vol. 7, no. 3/4, 2015.
- [68] S. Wang, S. Khatir, and M. Abdel Wahab, “Proper Orthogonal Decomposition for the prediction of fretting wear characteristics,” *Tribology International*, vol. 152, Article ID 106545, 2020.
- [69] D. Aleksendrić and Č. Duboka, “Fade performance prediction of automotive friction materials by means of artificial neural networks,” *Wear*, vol. 262, no. 7-8, pp. 778–790, 2007.
- [70] A. A. Sosimi, O. P. Gbenedor, O. Oyerinde, O. O. Bakare, S. O. Adeosun, and S. A. Olaleye, “Analysing wear behaviour of Al-CaCO₃ composites using ANN and Sugeno-type fuzzy inference systems,” *Neural Computing & Applications*, 2020.
- [71] F. Alambeigi, S. M. Khadem, H. Khorsand, and E. S. H. Mirza, “A comparison of performance of artificial intelligence methods in prediction of dry sliding wear behavior,” *International Journal of Advanced Manufacturing Technology*, vol. 84, no. 9-12, pp. 1981–1994, 2015.
- [72] A. ArriandiagaLaresgoiti, E. P. Portillo, J. A. G. Sánchez, I. A. Cabanes, and I. R. Pombo, “Virtual sensors for on-line wheel wear and part roughness measurement in the grinding process,” *Sensors*, vol. 14, no. 5, 2014.
- [73] A. Bustillo, D. Y. Pimenov, M. Matuszewski, and T. Mikolajczyk, “Using artificial intelligence models for the prediction of surface wear based on surface isotropy levels,” *Robotics and Computer-Integrated Manufacturing*, vol. 53, pp. 215–227, 2018.
- [74] R. E. Haber and A. Alique, “Intelligent process supervision for predicting tool wear in machining processes,” *Mechanics*, vol. 13, no. 8-9, pp. 825–849, 2003.
- [75] F. Aydin, “The investigation of the effect of particle size on wear performance of aa7075/al2o₃ composites using statistical analysis and different machine learning methods,” *Advanced Powder Technology*, vol. 32, no. 2, 2021.
- [76] G. O. Barrionuevo, J. A. Ramos-Grez, M. Walczak, and A. B. Carlos, “Comparative evaluation of supervised machine learning algorithms in the prediction of the relative density of 316L stainless steel fabricated by selective laser melting,” *International Journal of Advanced Manufacturing Technology*, vol. 113, no. 8, 2021.
- [77] M. Agarwal, M. Kumar Singh, R. Srivastava, and R. K. Gautam, “Microstructural measurement and artificial neural network analysis for adhesion of tribolayer during sliding wear of powder-chip reinforcement based composites,” *Measurement*, vol. 168, Article ID 108417, 2021.
- [78] M. Szala, M. Awtoniuk, L. Łatka, W. Macek, and R. Branco, “Artificial neural network model of hardness, porosity and cavitation erosion wear of APS deposited Al₂O₃-13 wt% TiO₂ coatings,” *Journal of Physics: conference Series*, vol. 1736, no. 1, Article ID 012033, 2021.
- [79] L. Tyagi, R. Butola, L. Kem, and M. S. Ranganath, “Comparative analysis of response surface methodology and artificial neural network on the wear properties of surface composite fabricated by friction stir processing,” *Journal of Bio- and Tribo-Corrosion*, vol. 7, 2021.
- [80] S. Basavarajappa, G. Chandramohan, and J. P. Davim, “Application of Taguchi techniques to study dry sliding wear behavior of metal matrix composites,” *Materials & Design*, vol. 28, no. 4, pp. 1393–1398, 2007.
- [81] Y. Sahin, “Optimization of testing parameters on the wear behavior of metal matrix composites based on the Taguchi method,” *Materials Science and Engineering: A*, vol. 408, no. 1-2, pp. 1–8, 2005.
- [82] V. E. Buchanan, P. H. Shipway, and D. G. McCartney, “Microstructure and abrasive wear behavior of shielded metal arc welding hardfacings used in the sugarcane industry,” *Wear*, vol. 263, no. 1-6, pp. 99–110, 2007.
- [83] C. S. Ramesh and A. Ahamed, “Friction and wear behavior of cast Al 6063 based in situ metal matrix composites,” *Wear*, vol. 271, no. 9-10, pp. 1928–1939, 2011.
- [84] H. Ahlatci, T. Koçer, E. Candan, and H. Çimenoglu, “Wear behavior of Al/(Al₂O₃p+SiCp) hybrid composites,” *Tribology International*, vol. 39, no. 3, pp. 213–220, 2006.
- [85] Y. Sahin and K. Özdin, “A model for the abrasive wear behavior of aluminium based composites,” *Materials & Design*, vol. 29, no. 3, pp. 728–733, 2008.
- [86] S. Basavarajappa, G. Chandramohan, A. Mahadevan, M. Thangavelu, R. Subramanian, and P. Gopalakrishnan, “Influence of sliding speed on the dry sliding wear behavior and the subsurface deformation on hybrid metal matrix composite,” *Wear*, vol. 262, no. 7-8, pp. 1007–1012, 2007.
- [87] K. Umanath, K. Palanikumar, and S. T. Selvamani, “Analysis of dry sliding wear behavior of Al6061/SiC/Al₂O₃ hybrid metal matrix composites,” *Composites Part B: Engineering*, vol. 53, pp. 159–168, 2013.
- [88] J. M. Durand, M. Vardavoulas, and M. Jeandin, “Role of reinforcing ceramic particles in the wear behavior of polymer-based model composites,” *Wear*, vol. 181–183, pp. 833–839, 1995.
- [89] J. Kondratiuk and P. Kuhn, “Tribological investigation on friction and wear behavior of coatings for hot sheet metal forming,” *Wear*, vol. 270, no. 11-12, pp. 839–849, 2011.
- [90] T. Sathish and S. Karthick, “Wear behavior analysis on aluminium alloy 7050 with reinforced SiC through taguchi

- approach,” *Journal of Materials Research and Technology*, vol. 9, no. 3, 2020.
- [91] P. Sharma, K. Paliwal, R. K. Garg, S. Sharma, and D. Khanduja, “A study on wear behavior of Al/6101/graphite composites,” *Journal of Asian Ceramic Societies*, vol. 5, no. 1, pp. 42–48, 2017.
- [92] S. A. Alidokht, A. Abdollah-zadeh, and H. Assadi, “Effect of applied load on the dry sliding wear behavior and the subsurface deformation on hybrid metal matrix composite,” *Wear*, vol. 305, no. 1-2, pp. 291–298, 2013.
- [93] M. Vrabel, I. Mankova, J. Beno, and J. Tuharský, “Surface roughness prediction using artificial neural networks when drilling udimet 720,” *Procedia Engineering*, vol. 48, pp. 693–700, 2012.
- [94] A. Leyland and A. Matthews, “On the significance of the H/E ratio in wear control: a nanocomposite coating approach to optimised tribological behavior,” *Wear*, vol. 246, no. 1-2, pp. 1–11, 2000.
- [95] F. Aydin and R. Durgut, “Estimation of wear performance of AZ91 alloy under dry sliding conditions using machine learning methods,” *Transactions of Nonferrous Metals Society of China*, vol. 31, no. 1, pp. 125–137, 2021.
- [96] P. Ramkumar, *Trends in Mechanical and Biomedical Design*, E. T. Akinlabi, P. Ramkumar, and M. Selvaraj, Eds., Springer, Singapore, 2021.
- [97] L. Provezza, I. Bodini, C. Petrogalli, M. Lancini, L. Solazzi, and M. Faccoli, “Monitoring the damage evolution in rolling contact fatigue tests using machine learning and vibrations,” *Metals*, vol. 11, 2021.
- [98] S. K. Pattnaik, A. Nayak, A. Parida, and S. S. Kumar, “The study of surface roughness and tool wear analysis in turning of aluminum using different advanced cutting tools (january 16, 2021),” in *Proceedings of the International Conference on Artificial Intelligence in Manufacturing & Renewable Energy (ICAIMRE)*, Bhubaneswar, India, October 2019.
- [99] C. S. Lee, Y. H. Kim, K. S. Han, and T. Lim, “Wear behavior of aluminium matrix composite materials,” *Journal of Materials Science*, vol. 27, no. 3, pp. 793–800, 1992.
- [100] B. Gülenç and N. Kahraman, “Wear behavior of bulldozer rollers welded using a submerged arc welding process,” *Materials and Design*, vol. 24, no. 7, pp. 537–542, 2003.
- [101] M. Semlitsch and H. G. Willert, “Clinical wear behavior of ultra-high molecular weight polyethylene cups paired with metal and ceramic ball heads in comparison to metal-on-metal pairings of hip joint replacements,” *Proceedings of the Institution of Mechanical Engineers - Part H: Journal of Engineering in Medicine*, vol. 211, no. 1, pp. 73–88, 1997.
- [102] K. Sivaprasad, S. K. Babu, S. Natarajan, R. Narayanasamy, B. A. Kumar, and G. Dinesh, “Study on abrasive and erosive wear behavior of Al 6063/TiB2 in situ composites,” *Materials Science and Engineering: A*, vol. 498, no. 1-2, pp. 495–500, 2008.
- [103] L. Natrayan and M. K. Senthil, “Optimization of wear behavior on AA6061/Al₂O₃/SiC metal matrix composite using squeeze casting technique – statistical analysis,” *Materials Today Proceedings*, vol. 27, 2019.
- [104] J. U. Prakash, T. V. Moorthy, and S. Ananth, “Fabrication and sliding wear behavior of metal matrix composites,” *Applied Mechanics and Materials*, vol. 612, pp. 157–162, 2014.
- [105] C. S. Ramesh, C. K. Srinivas, and B. H. Channabasappa, “Abrasive wear behavior of laser sintered iron–SiC composites,” *Wear*, vol. 267, no. 11, pp. 1777–1783, 2009.
- [106] A. Raj, S. R. Kishore, L. Jose et al., “A survey of electromagnetic metal casting computation designs, present approaches, future possibilities, and practical issues,” *Eur. Phys. J. Plus*, vol. 136, 2021.
- [107] G. Hermann, “Artificial intelligence in monitoring and the mechanics of machining,” *Computers in Industry*, vol. 14, no. 1-3, pp. 131–135, 1990.
- [108] S. K. Selvaraj, K. Srinivasan, U. Chadha et al., “Contemporary Progresses in ultrasonic welding of aluminum metal Matrix Composites,” *Frontiers in Materials*, vol. 8, Article ID 647112, 2021.
- [109] A. Sharma, A. Chouhan, L. Pavithran, U. Chadha, and S. K. Selvaraj, “Implementation of LSS framework in automotive component manufacturing: a review, current scenario and future directions,” *Materials Today Proceedings*, vol. 46, 2021.
- [110] R. Sivasubramani, A. Verma, G. Rithvik, U. Chadha, and K. S. Senthil, “Influence on nonhomogeneous microstructure formation and its role on tensile and fatigue performance of duplex stainless steel by a solid-state welding process,” *Materials Today Proceedings*, vol. 46, no. 5, 2021.
- [111] K. Virmani, C. Deepak, S. Sharma et al., “Nanomaterials for automotive outer panel components: a review,” *Eur. Phys. J. Plus*, vol. 136, 2021.
- [112] K. S. Senthil, R. Ramesh, M. Tharun et al., “New developments in carbon-based nanomaterials for automotive brake pad applications and future challenges,” *Journal of Nanomaterials*, vol. 2021, Article ID 6787435, 24 pages, 2021.
- [113] M. Dharnidharka, U. Chadha, L. M. Dasari et al., “Optical tomography in additive manufacturing: a review, processes, open problems, and new opportunities,” *Eur. Phys. J. Plus*, vol. 136, 2021.
- [114] T. Ghimire, A. Joshi, S. Sen, K. Chinmay, U. Chadha, and K. S. Senthil, “Blockchain in additive manufacturing processes: recent trends & its future possibilities,” *Materials Today Proceedings*, in Press, 2021.
- [115] S. D. Mamdiwar and Z. Shakrwal, “Recent advances on IoT-assisted wearable sensor systems for healthcare monitoring,” *Biosensors*, vol. 11, no. 11, p. 372, 2021.
- [116] T. Pati, P. H. Kabra, and U. Chadha, “Statistical quality study of the parts produced in an automobile industry: a Daimler India case study,” in *IOP Conference Series: Materials Science and Engineering*, vol. 1206, no. 1, Article ID 012022, 2021.
- [117] H. Unal and A. Mimaroglu, “Friction and wear behaviour of unfilled engineering thermoplastics,” *Materials & Design*, vol. 24, no. 3, pp. 183–187, 2003.